Final Report

Title: **Radiation measurements in simulated ablation layers**

AFOSR/AOARD Reference Number: AOARD-09-**4144**

AFOSR/AOARD Program Manager: Dr. R. Ponnappan

Period of Performance: 1 July 2009 – 30 June 2010

Submission Date: 30 November 2010

Principal Investigator: Richard Morgan
The University of Queensland

Report Documentation Page	Form Approved OMB No. 0704-0188

Public reporting burden for the collection of information is estimated to average 1 hour per response, including the time for reviewing instructions, searching existing data sources, gathering and maintaining the data needed, and completing and reviewing the collection of information. Send comments regarding this burden estimate or any other aspect of this collection of information, including suggestions for reducing this burden, to Washington Headquarters Services, Directorate for Information Operations and Reports, 1215 Jefferson Davis Highway, Suite 1204, Arlington VA 22202-4302. Respondents should be aware that notwithstanding any other provision of law, no person shall be subject to a penalty for failing to comply with a collection of information if it does not display a currently valid OMB control number.

1. REPORT DATE **06 DEC 2010**	2. REPORT TYPE **FInal**	3. DATES COVERED **01-08-2009 to 30-07-2010**

4. TITLE AND SUBTITLE **Radiation measurements in simulated ablation layers**	5a. CONTRACT NUMBER **FA23860914144**
	5b. GRANT NUMBER
	5c. PROGRAM ELEMENT NUMBER
6. AUTHOR(S) **Richard Gareth Morgan**	5d. PROJECT NUMBER
	5e. TASK NUMBER
	5f. WORK UNIT NUMBER
7. PERFORMING ORGANIZATION NAME(S) AND ADDRESS(ES) **The University of Queensland,Brisbane,,Queensland 4072,Australia,AU,4072**	8. PERFORMING ORGANIZATION REPORT NUMBER **N/A**
9. SPONSORING/MONITORING AGENCY NAME(S) AND ADDRESS(ES) **AOARD, UNIT 45002, APO, AP, 96337-5002**	10. SPONSOR/MONITOR'S ACRONYM(S) **AOARD**
	11. SPONSOR/MONITOR'S REPORT NUMBER(S)

12. DISTRIBUTION/AVAILABILITY STATEMENT
Approved for public release; distribution unlimited

13. SUPPLEMENTARY NOTES

14. ABSTRACT
In this study, radiation in ablating shocklayers over a scale Stardust model at 9 km/s was measured during the 80 μs steady test flow produced in a high enthalpy super-orbital expansion tunnel. The presence of an ablating shock layer when an epoxy coating is used with air and nitrogen test gases is shown by spectrometric and high speed camera data, and is in agreement with previous experimental results. Shock layer radiation is found to be strongest in the UV and visible portions of the electromagnetic spectrum, in both ablating and non-ablating shock layers. Shock layer radiation is greatly increased in ablating shock layers than in non-ablating shock layers when both air and nitrogen test gases are used. A nitrogen test gas is thought to produce a higher temperature shock layer than when air is used, implying that oxygen in air has a cooling effect on shocklayer radiation, due to the dissociation of the oxygen molecules which occurs. Shocklayer radiation in the near-IR is far weaker than that in the UV and consists of atomic, rather than molecular, transitions. As such, no distinct ablation layer is visible in the IR spectral data, however there is a doubling in radiance in the presence of an epoxy coating.

15. SUBJECT TERMS
Ablation, Thermal Environments, Reentry vehicles, Expansion tunnel

16. SECURITY CLASSIFICATION OF:			17. LIMITATION OF ABSTRACT	18. NUMBER OF PAGES	19a. NAME OF RESPONSIBLE PERSON
a. REPORT **unclassified**	b. ABSTRACT **unclassified**	c. THIS PAGE **unclassified**	**Same as Report (SAR)**	**27**	

Abstract

 The interaction between an ablating shocklayer and radiative heat transfer to a surface, such as occurs on an ablating hypervelocity re-entry vehicle, is poorly understood. Ablative products act as absorbers and emitters, the net effect of which is strongly dependent on gas composition, enthalpy and wavelength. This paper presents the results of an experimental study investigating radiation in an ablating shocklayer over a 1:13.5 scale Stardust forebody model in an expansion tunnel in air, and nitrogen atmospheres at 9 km/s. The model was coated with a low-pyrolysis temperature hydrocarbon coating, permitting its thermal decomposition and the release of carbon-containing gaseous species into the shocklayer within the 80 μs test time. Shocklayer radiation is visualised using a high speed camera, whilst the emission spectra along the stagnation streamline is measured with ultraviolet and infrared spectrometers. Evidence of coating ablation is presented and shown to produce an increase in radiation in the ultraviolet, in agreement with previous experimental results, and an increase in radiation in the infrared. The influence of oxygen in air is also investigated and found to have a cooling effect on the shocklayer, resulting in a decrease in shocklayer radiation and also shock standoff distance.

Objectives

The scientific objective of this project was to obtain ablating hypervelocity reentry flows in the laboratory, and to obtain emission spectrometery measurements from the radiating shock layers produced. The data can be used as a benchmark reference for the validation of ablation models and the associated numerical implementations. This will potentially enable spacecraft to be designed with more confidence and safety than before, and to minimize the mass of the thermal protection, without compromising structural integrity.

Introduction

The design of thermal protection systems (TPS) presents a critical challenge for hypervelocity flight (Gnoffo 1996, Munk 2002). The issue first arose in the 1950's when sustained supersonic flight became viable. Early solutions are illustrated by the well known pioneering vehicles the SR71 'Blackbird' and the Concorde. These vehicles incorporated 'hot structures' to balance aerodynamic heat loads, using radiative cooling within the thermal limits of titanium and aluminium respectively at Mach numbers up to 3.2. As flight speed increases, so too does the associated heat input, and more advanced techniques are needed to maintain structural viability. The X15 rocket plane used a combination of inconel and titanium hot structures at speeds up to Mach 7 to survive short durations of hypersonic flight.

In parallel with these developments, exploration of space required structures to survive speeds of up to 8 km/sec (Mach 25) for reentry from low earth orbit, and 11.2 km/sec (Mach 35) for return from the moon, and up to 47km/sec for Jupiter entry. Early designs were based on sacrificial ablative heat shields, where aerodynamic heating drives ablative products into the 'shock layer' of heated gas which surrounds the windward surfaces of hypersonic vehicles. These designs protect the structure of the space craft using the latent heat of the volatiles, through the insulating effect of the vapourised products surrounding the craft, and by radiative cooling from the carbon 'char' which is left behind after vapourisation. Many products have been successfully used for this purpose, including carbon phenolics (which form the basis of most sacrificial heat shields), cork and modern derivatives such as PICA and CSi coatings (Park 16, Laub 15).

Reusable thermal protection systems (TPS) have been developed for speeds of up to 8 km/sec (Mach 25), as exemplified by the US space shuttle. All missions requiring speeds higher than 8 km/s depend on ablative techniques, which form the focus of this application.

The mechanisms whereby ablative surfaces provide thermal protection are complex, and cannot be precisely modeled at present (Laux 2009). Current designs contain a large degree of empiricism, and generally use substantial safety factors to account for the unknown parameters. Surface ablation and phase change represent an extreme case of complex coupling between structural and aerothermodynamic

boundary conditions, with the interface between structure and fluid flow not being clearly defined. In addition, the ablation proceeds in the environment of a reacting non equilibrium shock layer, which in itself is also hard to characterise. The field lacks accurate experimental data, which makes it difficult to improve our theoretical understanding of the process, and to validate new models. Flight experiments are too expensive and time consuming to use for comprehensive research studies, and program managers are reluctant to include extra scientific instrumentation on reentry capsules as they may compromise the safety of the primary mission. The flight data we do have is very valuable, and remains the subject of study for many decades (Elbert 1993, Cauchon 1967, Corvette 1966, Ried 1972, Capra 2004 and 2007, Na 2008).

Ground testing of ablators is difficult. The impulsive facilities which are able to properly simulate the required flow conditions have insufficient run times to fully equilibrate the mass transfer processes involved. For instance, the exposed surface temperatures of an ablator are typically in the range of 2000 to 3000K, and contain a charred layer of carbon, with volatiles diffusing through to the shock layer from a receding and pyrolysing layer underneath. Time scales of the order of 1 to 10 seconds with heating rates in the range of 1 to 100 MWm^{-2} are required to establish quasi-steady conditions for this system. Arc jet facilities can achieve the required heat transfer rates for sustained periods of time, but do not properly simulate the surrounding hypervelocity flow field, nor its coupling with the ablative process. They are primarily useful for materials testing.

Recent developments in The University of Queensland expansion tunnels have demonstrated the ability to create a partial similarity with the flight situation. By exposing a thick layer of epoxy to a hypervelocity flow of 9 km/sec, it has been shown that a flow of ablative products can be established into the shock layer within approximately 20 microseconds. The ablative mixing layer has been probed by spectrometry and high speed photography, and is providing useful data for understanding the process and for evaluation of advanced theoretical models, (D'Souza 2010).

Analysis of the overall mechanisms of ablative protection can be broadly categorized into the following interacting stages and issues:

- Materials properties. These are complex and highly temperature and phase dependant, typically involving a composite material consisting of a matrix of fibres, impregnated with a volatile resin. Both the matrix and the volatiles may react chemically with the shock layer.
- Heat and mass transfer within the substrate, driven by aerodynamic heating.
- The non equilibrium external hypervelocity shock layer flow field.
- Diffusion and entrainment of the ablative products into the shock layer.
- Radiative processes involving the shock layer, the mixing layer which contains the ablated products, and the exposed surface of the heat shield.
- Chemical interaction between shock layer and ablative products

The first two processes are best studied using long duration facilities, with conditions set to reproduce the heat transfer rates to be expected in flight. The remaining processes are driven by and coupled to the external flow field, and are the target of this study. By creating a stream of ablative material into the shock layer, the external flow processes can be studied independently of the internal mass and heat transfer mechanisms which are involved in a flight situation.
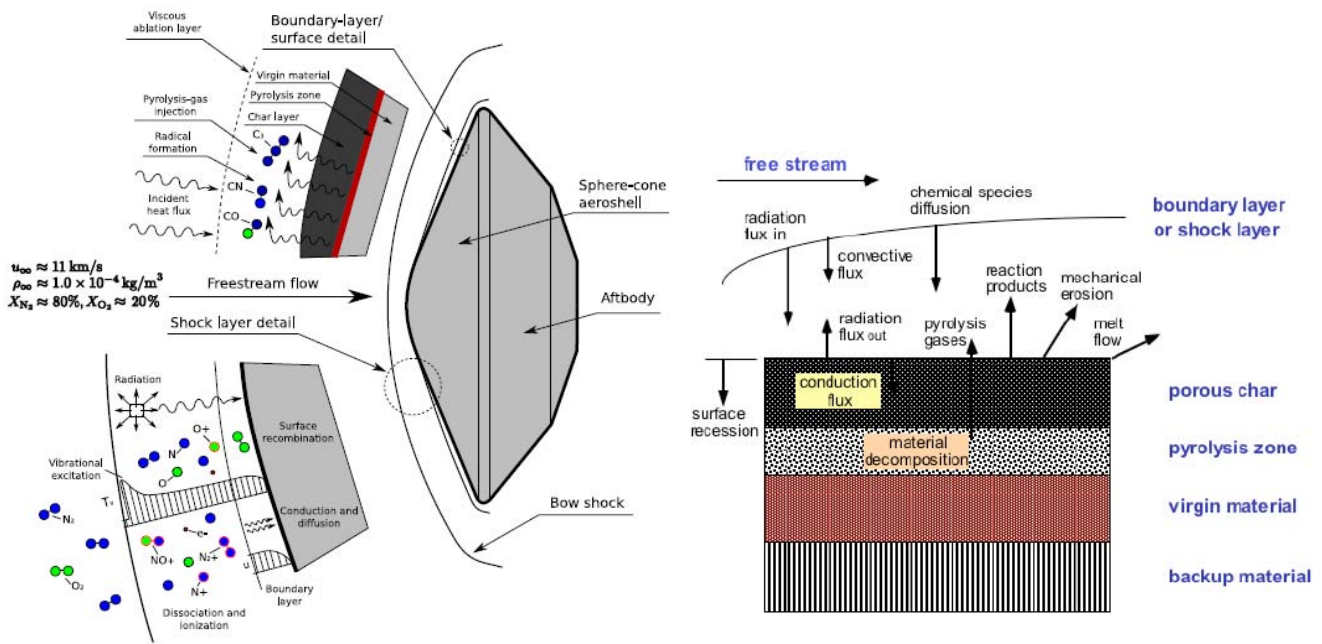
Schematic of processes involved in an ablative TPS shock layer in air. (Laub 2008)

Immediately behind the bow shock is a region of non equilibrium chemistry and radiation, which is currently being studied in a related Australian Research Council Discovery project, DP 1094560. At Reynolds numbers of most interest, this region will be physically separated from the ablative mixing layer adjacent to the windward surface of the vehicle. However, it is coupled to it through radiation, and the entrainment of gas which passes from this region into the mixing layer. Uncertainties in this region relate to the post shock chemical kinetics, the associated non equilibrium radiation and the coupling of these processes with the rest of the flow field.

The mixing layer itself is characterised by the entrainment of ablated products from the wall into the hypervelocity boundary layer. This may be in the form of vapourised or sublimated volatiles (primarily some form of hydrocarbons), carbon particulates, and a variety of specific additives such as silicon compounds which may be present in the ablator. The mixing layer is also a region of extreme non equilibrium activity, and a participant in radiative processes (either as a transmitter, absorber or source). Hydrocarbons in the mixing layer break down to lighter species thereby absorbing thermal energy, and react with entrained freestream species either endo or exo-thermically. The high carbon content of the ablators leads to the formation of a variety of C species which are typically strong radiators if they get hot enough, such as CN and CO, (Park 2007).

Poorly understood processes in the mixing layer include the non equilibrium chemical kinetics and associated radiation, and the influence the mass addition has on the development of the mixing layer and the associated level of turbulence. The rate of mass release is driven by surface heat transfer, which is hard to predict, as it is dominated by radiation and convection through the mixing layer itself.

Future spacecraft returning from the Moon, Mars and beyond will re-enter the Earth‟s atmosphere at speeds faster than ever before. The Stardust sample return spacecraft was the fastest successful re-entry of an artificial hypervelocity, entering Earth‟s atmosphere at a speed of 12.8 km/s in January 2006, Jeniskens 2005. Due to its successful re-entry, future hypervelocity sample return spacecraft will be modelled on the Stardust spacecraft. Atmospheric entry at these hypervelocity speeds, typically above 12 km/s, results in extreme heating of the spacecraft. The only thermal protection systems capable of protecting hypervelocity spacecraft are ablative TPS. Whilst the interaction between an ablating TPS and convective heat transfer is understood, little is known of the effect of ablation on radiative heat transfer. As a result, ablative TPSs are typically oversized, sometimes by up to four times, Milos 1997. In order to optimise spacecraft mass to allow maximum mass allocation to the scientific payload whilst providing adequate thermal protection, an improved understanding of the effect of ablation on radiation is desired.

No instrumentation was carried onboard the Stardust SRC for the re-entry phase of the mission. The only available flight data was captured from an airborne observatory, and is limited to spectra of the entire shocklayer without spatial resolution, Winter 2007. Although not verified either in flight or ground tests, several computational predictions have also been developed, Johnston 2007,Olyniack 1999, Park 2007. Present work consists of ground testing of radiation from ablating shocklayers in hypersonic flows to enable verification of computational codes.

The ground-based test facilities most closely able to replicate the high enthalpy, chemically reacting shocklayers characteristic of super-orbital re-entry flows are expansion tube facilities, Morgan2006. These are impulse facilities with brief, steady test periods of the order of 50 to 500 μs. However, ablation is a chemical and physical phenomenon requiring prior heating, previously considered to be of the order of minutes. Outgassing associated with ablation is known to contaminate the test conditions within an expansion facility, thereby rendering ablation simulation in expansion facilities difficult. Ablation simulation in expansion facilities had therefore been limited to a subset of ablative heat shield phenomena, such as gaseous product effusion from the forebody surface during the brief steady test time, Morgan 1999, and simulation of a pre-heated graphite layer, Hunt 2002.

Proof-of-concept experiments have demonstrated that a low-pyrolysis temperature hydrocarbon (epoxy) coating may be used to study ablation in impulse facilities, D'Souza 2010. Radiating, carbon-containing ablative material, arising from pyrolysis of an epoxy coating, is used to simulate an ablating TPS.

This paper presents a summary of the experimental work conducted in expansion facilities at The University of Queensland on the interaction between an ablating shocklayer and radiative heat transfer around a Stardust scale model forebody. Test gases used are air and nitrogen. The epoxy coating employed in this work is „Five Minute Araldite‟ (®Huntsman Corporation). High speed camera and spectrometric results show ablation of the coating, in agreement with previous findings. The results of investigations into the effect of various test gases with wavelength are presented here.

ANALYSIS

A 1D semi-infinite analysis was performed to demonstrate that vaporisation of an epoxy coating is possible within the brief test times available in expansion facilities. Conditions taken in the analysis of the heat flux to the epoxy coating are given in Table 1. The Zoby stagnation point heat flux approximation for convective heat flux to the (cold) nose of the model (Eq. 1, Zobt 1968) is used in conjunction with the Schultz and Jones temperature change for a constant heat flux during the exposure time (Eq. 2, Schultz and Jones 1973):

(1) $\dot{q}_S = K_i \sqrt{\rho u^2} \dfrac{u^2}{\sqrt{r_{eff}}}$

(2) $\Delta T_S = \dfrac{2\dot{q}_S}{\sqrt{\pi}} \sqrt{\dfrac{t}{\rho c k}}$

This provides a conservative estimate for the epoxy surface temperature change, as the effect of radiative heat flux is ignored. A surface temperature change for epoxy of 158 K in 50 μs is calculated, which is adequate for epoxy to commence ablation in the form of outgazing, with no surface chemistry.

Application of the Schultz and Jones 10% step function thermal pulse penetration depth approximation for insulating materials (Eq. 3, Schultz and Jones 1973) finds the depth at which the epoxy temperature is 10% of the value at the surface is 6 μm in 50 μs. As this is much smaller than the 1.5 mm thick epoxy coating, the model nose surface curvature can be neglected, enabling the 1D semi-infinite analysis of the heat flux to the coating and its ablation behaviour.

$$(3) \quad x = 2x^* \sqrt{\alpha t}$$

Chemical analyses performed on epoxy to determine its pyrolysis temperature and gas composition were conducted using a residual gas analyser (RGA) and thermogravimetric analyser (TGA). Both instruments conducted testing at different conditions to those experienced in expansion facilities: 90 μPa vacuum with a helium carrier gas and 20 K/min furnace heating rate in the RGA, and a 10 K/min heating rate in nitrogen atmosphere in the TGA compared with the 341 Pa vacuum in air and thermal shock heating condition in the X2 expansion tunnel. Results from the RGA indicate epoxy pyrolysis gases consist primarily of carbon monoxide, carbon dioxide, methane and water vapour. The epoxy pyrolysis temperature is similar for both instruments: 613 K in the RGA and 598 K in the TGA.

Parameter	Value	Reference
Test gas density, g/m^3	0.532 ± 0.150	8
Test gas speed, m/s	9000 ± 400	Present work
Effective nose radius, mm	16.2 ± 0.5	Present work
Exposure time to heat flux, μs	50 ± 1	Present work
Epoxy density, kg/m^3	1260 ± 150	16
Epoxy specific heat, J/kg/K	2110 ± 150, at 473 K	16
Epoxy thermal conductivity, W/m/K	0.188 ± 0.002	17
Epoxy alpha, m^2/s	$(1.7 \pm 0.8) \times 10^{-7}$	Present work
Epoxy sublimation temperature, K	630 ± 10	Present work
x^*	1	13
Zoby stagnation point heat flux, MW/m^2	14.97 ± 0.02	12, present work
Temperature change, K	178 ± 1	13, present work
10% temperature penetration depth, μm	6.0 ± 0.5	13, present work
1% temperature penetration depth, μm	21 ± 3	13, present work

Table 1: Conditions taken in the analysis of heat flux to the epoxy coating

DESCRIPTION OF EXPERIMENTS
Experimental Conditions
The University of Queensland expansion facility used for this study is the X2 free-piston driven, high-enthalpy facility. X2 was used in expansion tunnel mode for these experiments, as shown in Figure 1. Air and nitrogen 47.1 MJ/kg, 9 km/s test gas conditions were used in this study. Experimental parameters and computed freestream conditions are given in Table 2.
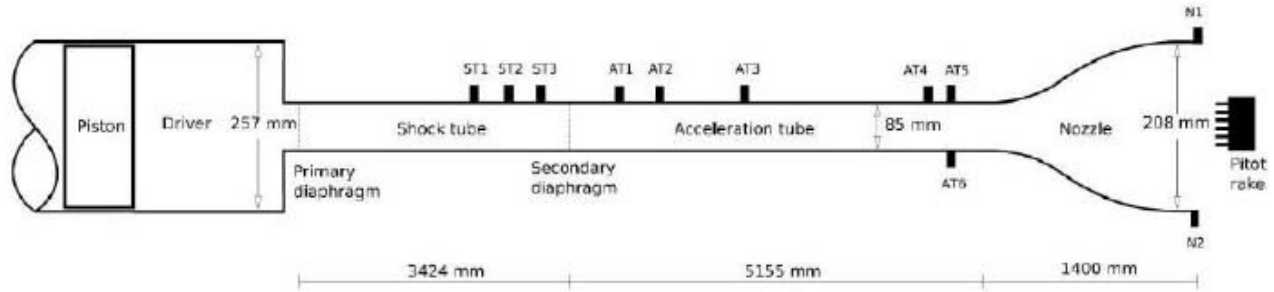
Fig. 1: Schematic of X2 expansion facility operated in expansion tunnel mode.

Parameter	Air	Nitrogen
EXPERIMENTAL PARAMETERS		
Measured shock speeds		
Primary shock, m/s	5000 ± 200	5000 ± 200
Secondary shock, m/s	9000 ± 400	9000 ± 400
Measured freestream conditions		
Pitot pressure, kPa	155 ± 15	125 ± 15
Test time, µs	80	80
COMPUTED FREESTREAM CONDITIONS		
Total enthalpy, MJ/kg	47.1 ± 2.3	47.1 ± 2.3
Flight velocity, m/s	9788 ± 50	9788 ± 50
Pressure, Pa	654 ± 113	654 ± 113
Density, g/m^3	1.73 ± 0.32	1.73 ± 0.32
Temperature, K	$T_{tr}\ 1069 \pm 54$	$T_{tr}\ 1069 \pm 54$
	$T_{ve}\ 1202 \pm 70$	$T_{ve}\ 1202 \pm 70$
Mole fractions		
$X[N_2]$	$6.27 \pm 0.11 \times 10^{-1}$	$9.06 \pm 0.5 \times 10^{-1}$
$X[N_2^+]$	$1.16 \pm 0.5 \times 10^{-7}$	$2.00 \pm 0.5 \times 10^{-5}$
$X[NO]$	$2.18 \pm 0.17 \times 10^{-4}$	0.00
$X[NO^+]$	$7.24 \pm 1.40 \times 10^{-5}$	0.00
$X[O_2]$	$5.75 \pm 1.44 \times 10^{-3}$	0.00
$X[O_2^+]$	$2.23 \pm 0.5 \times 10^{-7}$	0.00
$X[N]$	$3.63 \pm 0.80 \times 10^{-2}$	$9.36 \pm 0.5 \times 10^{-2}$
$X[N^+]$	$2.70 \pm 0.5 \times 10^{-8}$	$9.54 \pm 0.5 \times 10^{-6}$
$X[O]$	$3.30 \pm 0.00 \times 10^{-1}$	0.00
$X[O^+]$	$2.78 \pm 0.5 \times 10^{-7}$	0.00
$X[e^-]$	$2.50 \pm 0.45 \times 10^{-16}$	$7.66 \pm 0.5 \times 10^{-10}$
$X[CO_2]$	-	-
$X[CO]$	-	-
Mach number	12.5 ± 0.3	12.5 ± 0.3
Unit Reynolds Number, m^{-1}	1.25×10^5	1.25×10^5

Table 2: X2 9 km/s air and nitrogen test gas condition experimental parameters and computed freestream conditions in test section. The computed freestream condition for air takes air as consisting of 76.7% N_2 and 23.3% O_2.

Freestream conditions are calculated using an analysis derived from the results of previous studies, Potter 2008, in which detailed simulations of the secondary diaphragm rupture process with both thermal and chemical non-equilibrium were performed. Quasi-1D Lagrangian simulations of the air condition considered in this paper (Table 2) with chemical non-equilibrium and an inertial diaphragm model were performed in

[8]. The freestream composition at the nozzle exit was found to be approximately frozen at the shock processed composition in the shock tube:

$$X_{i,\infty} \approx X_{i,shock\_tube} \qquad (4)$$

As a result, the present work uses the NASA CEA program, Gordon, S. & McBride, B.J. (1994) to calculate the shock tube composition and set this result as the freestream composition. The high speed, low density shock tube condition causes the accelerator-test gas interface to catch up with the secondary shock wavem as described by Mirels, 1960. The freestream velocity is therefore well approximated by the secondary shock speed due to the low acceleration tube pressure and high secondary shock speed:

$$u_{\infty} \approx U_{s,2} \qquad (5)$$

The freestream pressure is measured by the nozzle static transducers in the experiment:
The freestream density is calculated based on the experimentally measured Pitot and static pressures:

$$P_{pitot,\infty} \approx \rho_{\infty} u_{\infty}^2 \qquad (7)$$

$$\therefore \rho_{\infty} \approx \frac{P_{pitot,\infty}}{u_{\infty}^2} \qquad (8)$$

The freestream is assumed to be in thermal equilibrium, thereby permitting the freestream temperature to be calculated from the equation of state:

$$T_{\infty} = \frac{P_{\infty}}{\rho_{\infty} R_{\infty}} \qquad (9)$$

This procedure is based on the experimentally measured shock speed and pressure levels, and has been shown to give a good estimate of the flow conditions.

Model

The model used in this study is a 1:13.5 scale mild steel 60° sphere-cone with a 60 mm base radius and nose-to-base radius ratio of 0.54. For the ablating surface tests, various portions of the forward surface of the model were coated with epoxy, allowed to cure and then machined to a 1.5 mm thickness with the same shape and outside diameter of the original steel forward surface, as shown in Fig. 2. Skirt-coated models had epoxy applied to the conical segment of the forebody, whilst nose-coated models had epoxy applied to the spherical segment.
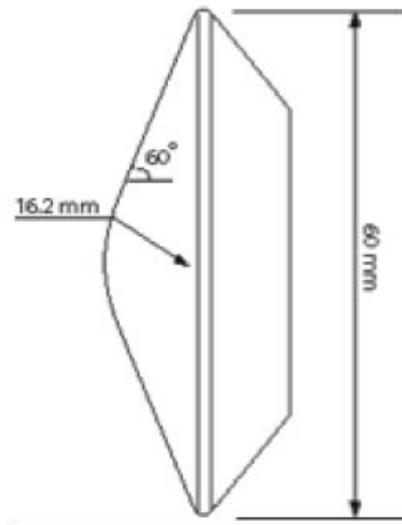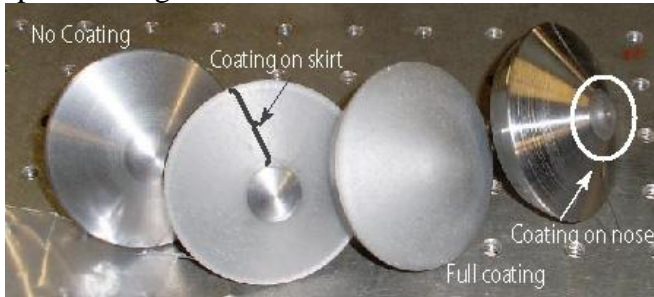

Fig. 1   Stardust Models. L-R: No Coating; Coating on Skirt; Full Coating; Coating on Nose.

Optical Instrumentation

Luminosity from substantial portions of the model and shocklayer flow was visualised using a Shimadzu HPV1 high-speed charge-coupled device (CCD) video camera recording at 500 kfps with a 1 µs exposure time. Radiation from chemical species in a narrow, 3.9 mm long strip of the field of view parallel to and including the stagnation streamline was spectrally resolved using two Acton Research SpectroPro 2300i spectrographs fitted with 600 line/mm diffraction gratings blazed at 300 nm and 500 nm, coupled to a Princeton Instruments PI-max image intensified CCD camera and optimised for sensitivity in the UV (UV spectrograph) and visible/near IR (IR spectrograph). Radiation was collected across the field of view and integrated over a 10 µs interval midway through the 80 µs steady test flow period. Mirrors used in the optical paths were UV enhanced aluminium (UV spectrograph), aluminium (high speed camera) and silver (IR spectrograph). The optical set-up is illustrated in Figure 3.
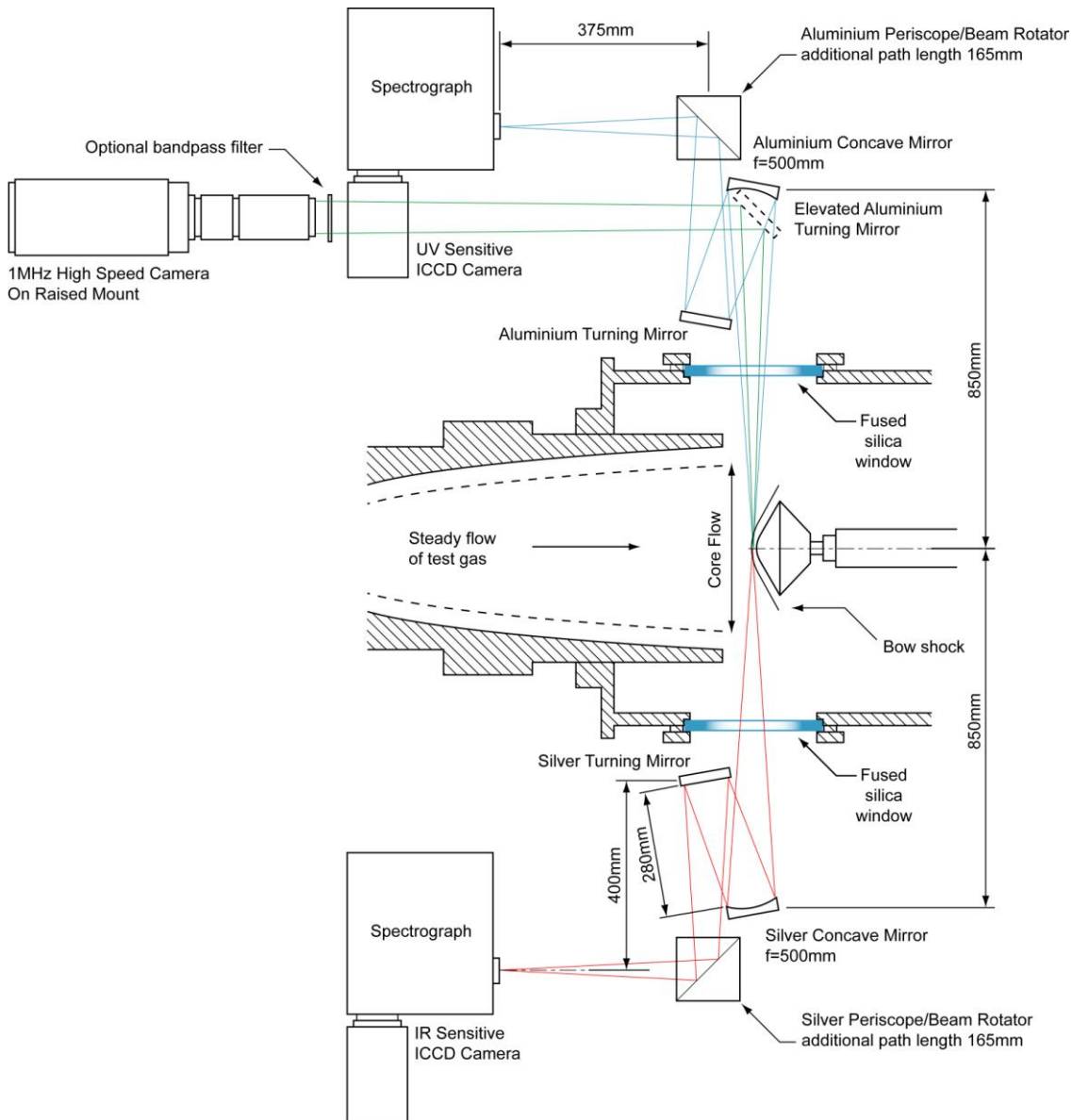
Fig. 2   X2 Test Section Schematic.

Calibration of the response of the ICCD cameras was conducted by measuring the counts received from a calibrated light source of known spectral irradiance placed in front of the spectrograph. The camera

response can be re-interpreted in terms of spectral irradiance after accounting for the detector sensitivity, the transmittance or reflectance of the various optical components, the limiting aperture and the optical power of the arrangement. The calibration is then converted to spectral radiance and compared to the spectra observed in the experiments.

HPV1 High Speed Camera

A negative greyscale image of the model with and without an epoxy coating produced by the HPV1 is shown in Figure 4. This image is taken approximately 60 μs into the 80 μs steady test period. In those parts of the shock layer forward of the model upper edge when no coating is present, a nearly uniform signal is observed. An additional glowing layer, approximately 0.2 mm thick, is observed along the model upper edge when an epoxy coating is used. The glowing layer is believed to be an ablation layer, that is, a region in the shock layer where the high concentrations of ablation products emanating from the coating meet the oncoming flowfield, D'Souzq 2010. At approximately 20 μs after the arrival of the starting shock and 30 μs before the start of the steady test period, the ablation layer first appears. The ablation layer is visible throughout the steady test period, increasing in luminosity though not in thickness.

The shocklayer can be argued to be optically thin both with and without an epoxy coating present on the model, as the model surface appears less luminous than the region of the shocklayer visible above the model edge. Abel transformation of the HPV1 images reveals that the radiative power density is high immediately behind the shock and decreases rapidly as the model surface or ablation layer is approached, as presented in Figure 5. In the epoxy coating case (Figure 5b), the radiative power density rises from its low point in the middle of the shocklayer to reach a second peak in the ablation layer.

UV Spectrometer

UV emission spectra from the ablation layer (a 12 pixel high strip on the centreline, 0.067 – 0.267 mm from the stagnation point) in the 340 – 440 nm wavelength range is shown in Figure 6, alongside the emission spectra in the same region, in a non-ablating shock layer. The dominant source of shock layer luminosity is cyanogen (CN, violet transitions) in the 250 – 550 nm wavelength range. Cyanogen is mostly formed by the reaction

$$N_2 + C \rightleftharpoons CN + N \qquad [11]$$
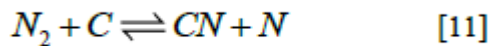
In all shots, the CN is present immediately behind the bow shock in both uncoated and coated model shots. For both air and nitrogen test gas flows without an epoxy coating, the source of carbon for CN production via reaction is thought to originate from contamination in the test gas, the origins of which could be the Mylar secondary diaphragm, graphite grease, buffer materials and even the remains of epoxy coating debris from previous shots. Attempts were made to clean the tunnel between shots in the experimental program to reduce this contamination, however these efforts made little difference to the observed signal strength.

A strong increase in CN violet and C2 radiation is observed in the ablation layer in air and nitrogen test flows when an epoxy coating is employed, in agreement with previous experimental results, D'Souza 2008. This is thought to arise from the mixing and reaction of carbon-rich gaseous ablation products with nitrogen from the shocklayer gas to produce CN. C2 Swann band emission is observed in the air and nitrogen test flows, although only for the epoxy coated model shots and only in the ablation layer. This reinforces the view that the epoxy coating is ablating, producing carbon-rich ablation products in the process and, in this way, providing carbon for CN production in the ablation layer.

As the thermal boundary layer at the model surface of the blunt body model can only be cooler than the forward regions of the shocklayer, this implies an increase in CN emission may only occur in and around the thermal boundary layer through increases in CN concentration. Increases in CN concentration are brought about by chemical reactions in that region, further supporting the argument that an ablation layer is present when an epoxy coating is used in air or nitrogen test gas flows.

The radiative emissions for an epoxy coated model in a nitrogen test flow are approximately 15% higher in the ablation layer than in an air test flow. This may be due to oxygen dissociation in the air freestream as well as further dissociation in the shocklayer leading to cooler conditions and therefore generally lower

emissions. This may also be due to higher N radical concentrations available for CN production in the ablation layer in the nitrogen test flow shocklayer either due to the higher flow temperatures and/or due to N radical reduction through competition with reactions consuming N and O.

The Ca+ atomic lines observed in Figure 6 are contaminant lines observed regularly when the X2 expansion facility is operated in expansion tunnel mode. The Ca+ atomic lines are stronger when no coating is employed in an air test gas, implying some Ca+ contamination arises from the steel model itself, which is consistent with previous findings, Buttsworth 2010. Interestingly, the contaminant Ca+ atomic lines are slightly increased in a nitrogen environment with an epoxy coating, and significantly increased in a nitrogen environment without a coating. This further suggests that a nitrogen test gas provides a higher temperature shock layer than air.

Estimates of ablation layer transitional and vibrational temperatures using second-order spectral lines in conjunction with the SpecAir radiation spectra program, Laux 2006 (not shown here) give ablation layer temperatures of 8700+- 500 K when air is used as the test gas. This is significantly greater than the model wall temperature, hence the difference between experiment and flight equilibrium wall temperatures may not seriously affect the heat flux analysis.

IR Spectrometer

The IR emission spectra averaged across the entire shocklayer in the 815 – 875 nm wavelength range is shown in Figure 7 for air, both with and without an epoxy coating. In this wavelength region, little molecular structure is visible, with the emission spectra being composed primarily of atomic O and N lines. Despite this, the shocklayer radiance with an epoxy coating is approximately double that when no coating is used.

Comparison of Measurements

Measurements of the bow shock radiation distribution from radiating species in the shock layer from the UV spectrometer are shown in Figure 8 with and without an epoxy coating for the region of the stagnation streamline monitored by the spectrometer. The spectrometric data is averaged over the most luminous portion of the emission spectrum, primarily the CN violet $\Delta v = 0$ band between 374 and 390 nm.

The UV spectrometer shows the signal produced by the radiating species rises rapidly across the shock and then declines gradually with streamwise distance along the sampled shocklayer strip in the absence of an epoxy coating, regardless of test gas. This is consistent with a non-ablating, axisymmetric shocklayer with a high irradiance layer immediately behind the shock and a rapid decrease in irradiance toward the model surface.

In both air and nitrogen test gases, the shock stand-off distances (1.5 mm for air, 1.3 mm for nitrogen) are increased when an epoxy coating is present, compared with 1.1 mm for both gases without a coating. The increase in shock stand-off distance with an epoxy coating is expected, as epoxy has been shown to ablate in air and nitrogen test gases, and an ablating shocklayer is known to have an increased shock stand-off distance. This is because the shock "sees" the injected material over the body in a supersonic flow as the body itself, thereby causing the shock to increase its stand-off distance in proportion [20]. Without an epoxy coating, shock stand-off distances are similar for air and nitrogen test gases. Future analysis will examine the cause of this behaviour.

Measurements of the bow shock radiation distribution from both UV and IR spectrometers are shown in Figure 9 in air, with and without an epoxy coating. In the case of no coating, both spectrometers observe a rapid increase in spectral radiance across the shock, followed by a gradual decline with streamwise distance. This is as expected for a non-ablating axisymmetric shocklayer. In the case of an epoxy coating, however, similar radiation distribution shapes are not observed. Whilst the UV spectrometer measures a second peak near the model surface (the ablation layer), the IR spectrometer does not. This is as expected from earlier results – that the dominating radiating species are CN violet transitions which radiate in the UV and not in the IR. The IR spectrometer observes only atomic species when an epoxy coating is used in air. These species peak in radiance immediately behind the shock, then decline gradually with streamwise distance.

The behaviour of the shock stand-off distances in Figure 9, however, are not as expected. The IR spectrometer records a similar shock stand-off distance for both epoxy and no epoxy cases. This result is not expected, and is most likely due to poor focussing of the IR ICCD camera, causing difficulty in determining the exact shock and/or model position.

Although post-test measurements of the model would be desirable to determine definitively whether epoxy ablation has occurred, highly turbulent post- test time conditions in the expansion tunnel lead to further ablation as well as severe damage to the model. For this reason, post-test visual examination of the epoxy for material degradation, and shadowgraph or scale measurements to determine epoxy surface regression are not valid. The occurrence of ablation during the test time can only be measured by recording data during this period. Data from three independent instruments used in this study, the high speed camera, UV and IR spectrometers, suggest ablation is present when an epoxy coating is used in air and nitrogen test gases.

Additional studies of radiation from ablating shocklayer flows have been conducted in the expansion tube facility at The University of Queensland, following earlier proof-of-concept experiments showing the successful production of an ablating, radiating shock layer from an epoxy coating during the brief steady test time available.

In this study, radiation in ablating shocklayers over a scale Stardust model at 9 km/s was measured during the 80 µs steady test flow produced in a high enthalpy super-orbital expansion tunnel. The presence of an ablating shock layer when an epoxy coating is used with air and nitrogen test gases is shown by spectrometric and high speed camera data, and is in agreement with previous experimental results. Shock layer radiation is found to be strongest in the UV and visible portions of the electromagnetic spectrum, in both ablating and non-ablating shock layers. Shock layer radiation is greatly increased in ablating shock layers than in non-ablating shock layers when both air and nitrogen test gases are used.

A nitrogen test gas is thought to produce a higher temperature shock layer than when air is used, implying that oxygen in air has a cooling effect on shocklayer radiation, due to the dissociation of the oxygen molecules which occurs.

Shocklayer radiation in the near-IR is far weaker than that in the UV and consists of atomic, rather than molecular, transitions. As such, no distinct ablation layer is visible in the IR spectral data, however there is a doubling in radiance in the presence of an epoxy coating.
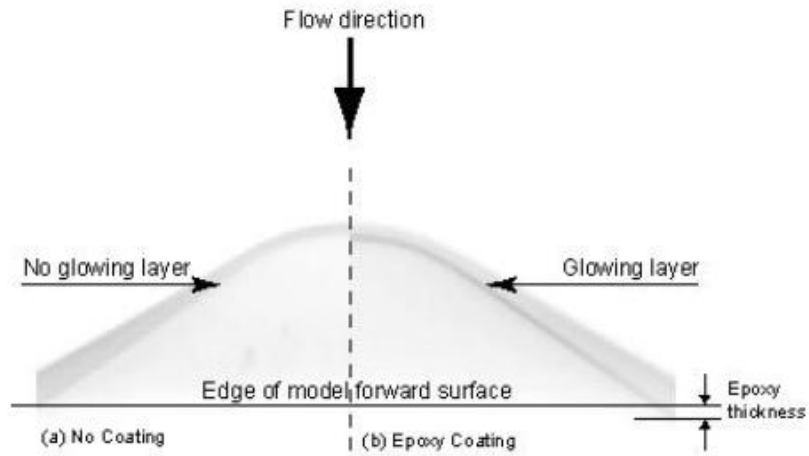
Fig. 4: Negative greyscale image of high speed camera footage 60μs after shock arrival in air test gas: a) no coating and b) epoxy coating.
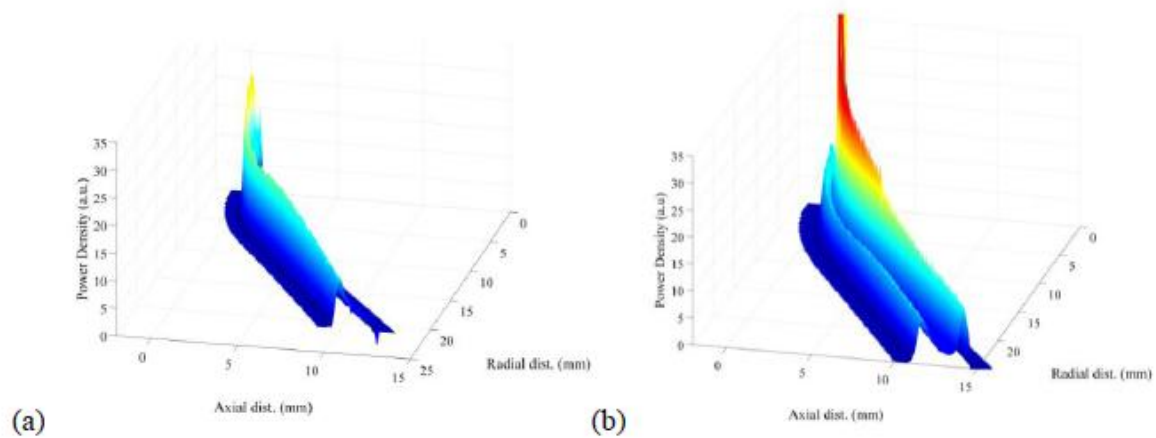

(a)

(b)

Fig. 5 Abel transformation of HPV1 image of nitrogen flow over a Stardust model: a) Steel model, power density at 48 us after shock arrival (x2s1234); b) Epoxy coated model, power density at 56 us after shock arrival (x2s1235).
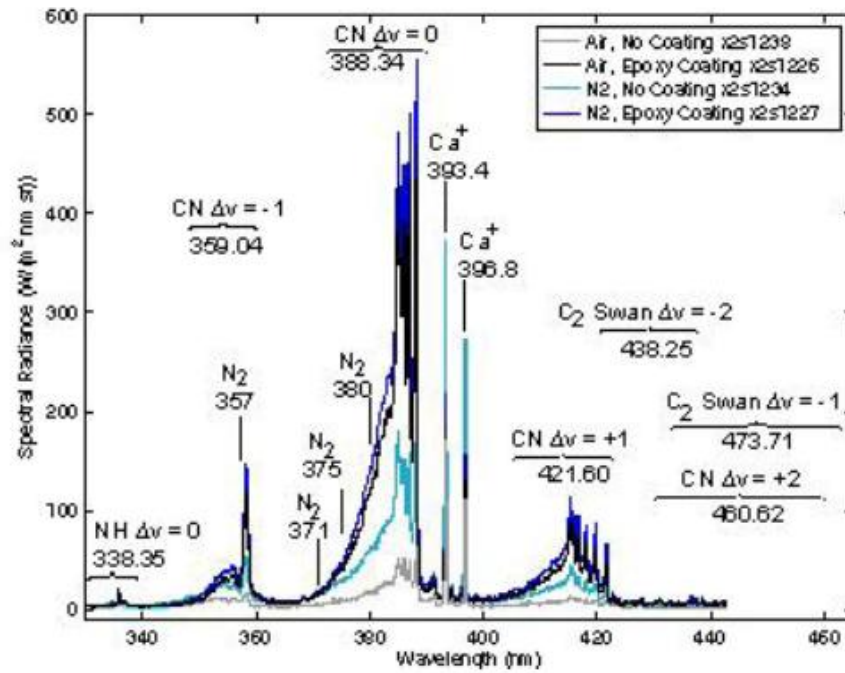
Fig. 6: Spectral irradiance measured on centreline, averaged in ablation layer 0.06-0.026 mm from stagnation point by UV spectrometer using 600 line/mm grating centred at 380 nm with air and nitrogen test gases.
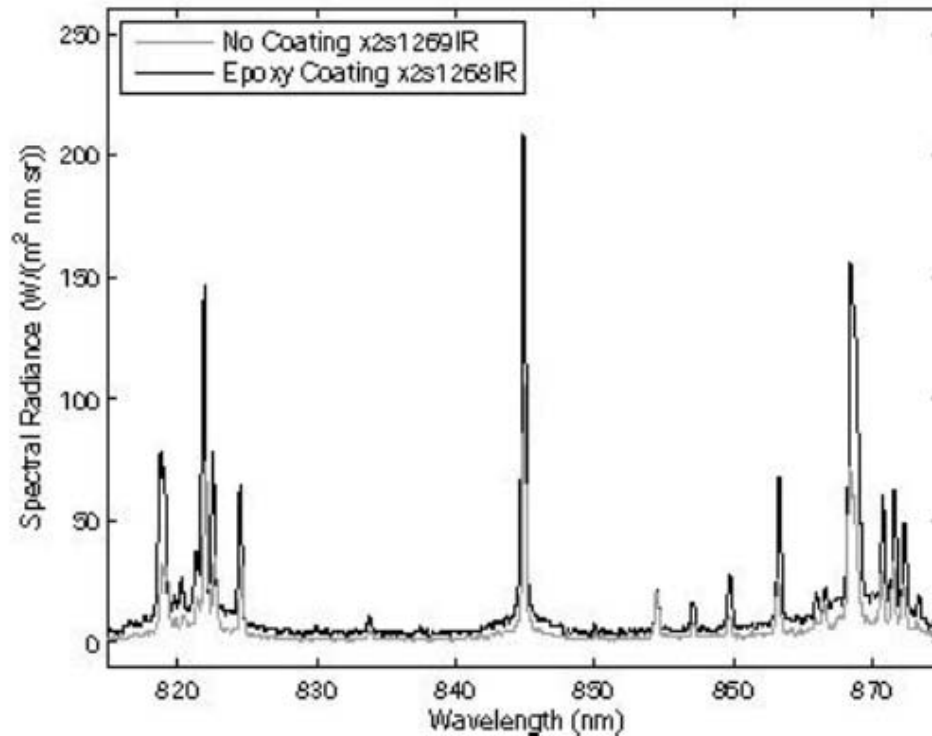

Fig. 7: Spectral irradiance measured on centreline, averaged in shocklayer by IR spectrometer using 600 line/mm grating centred at 850 nm in air.
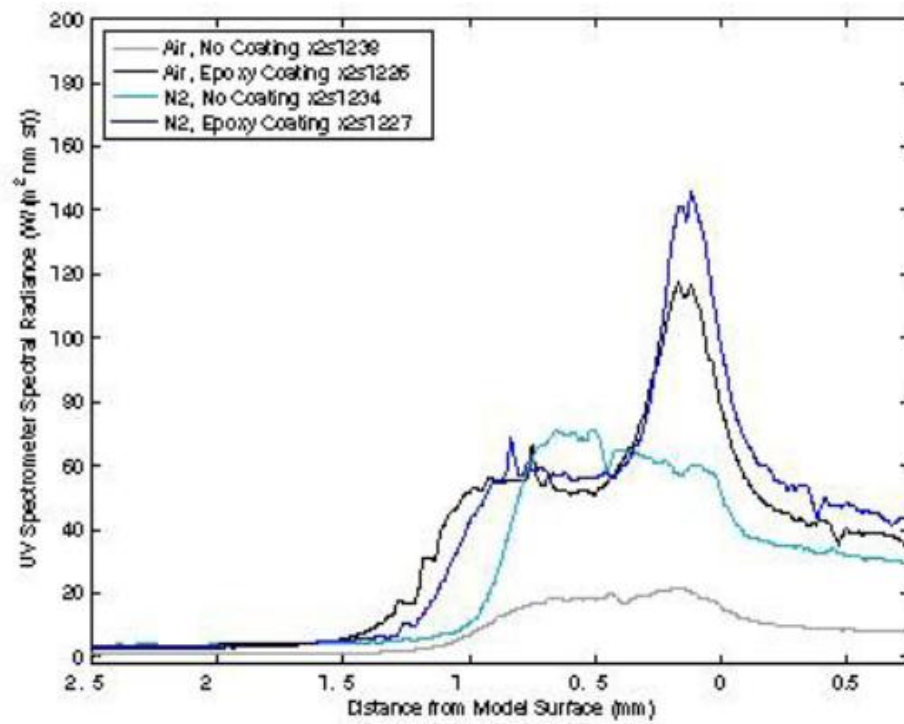
Fig. 8: Distribution of shocklayer radiation measured along the stagnation streamline in range 374 – 390 nm by the UV spectrometer using 600 line/mm grating centred at 380 nm with air and nitrogen test gases
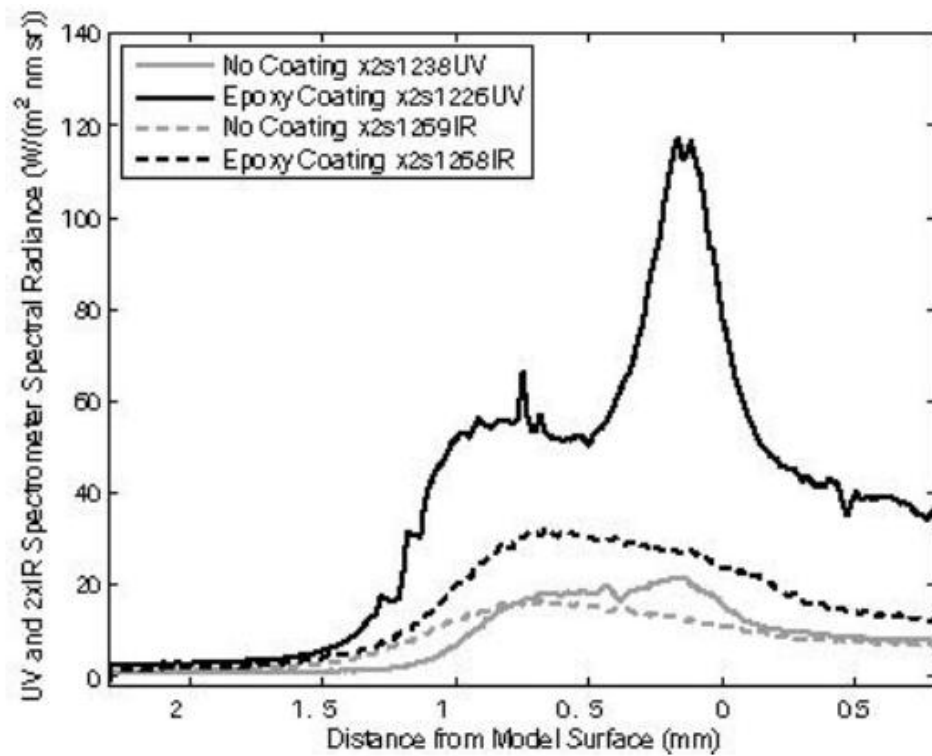
Fig. 9: Distribution of shocklayer radiation measured along the stagnation streamline by UV and IR spectrometers using 600 line/mm gratings centred at 380 nm (UV) and 850 nm (IR) in air. The UV spectrometer curves show radiation in the range 374 – 390 nm whilst the IR spectrometer curves are doubled for clarity and show radiation in the range 815 – 880 nm.

The bow shock radiation distribution as observed by both spectrometers with and without an epoxy coating is given in Fig. 10. Data from the IR spectrometer is increased by a factor of 10 for clarity. Due to its significant luminosity, an average of the emission spectra in the brightest region observed by the UV spectra, 374 - 390 nm, is displayed. The range observed by the IR spectrometer is 800- 900 nm. The high speed camera is most sensitive between 400 and 700 nm.

The shock standoff distance is greater when an epoxy coating is employed, as observed by the UV and IR spectrometers. This is consistent with findings by Kattari 1965, that the shock "sees" the injected gas over a body in a supersonic flow as the body itself and increases its standoff distance in proportion.

The shape of the bow shock radiation distribution observed by the UV spectrometer is quite different to that observed by the IR spectrometer. The UV spectrometer observes a strong ablation layer peak, peaking at 180 W/(m^2 nm sr) when an epoxy coating is employed, and a roughly uniform shock layer radiance of around 20 W/(m^2 nm sr) when no coating is employed.

However, the IR spectrometer radiation distribution slowly peaks behind the shock and gradually decreases as the model is approached. There is little difference in shape between the radiation distributions with and without an epoxy coating, implying that ablation layer radiance is strongest in the UV and visible spectral regions. This is consistent with observations of maximum spectral radiance over 21 times greater in the UV

than that in the IR. The IR epoxy coating case reaches a maximum spectral radiance of 8.5 W/(m^2 nm sr) in the shocklayer, whilst the IR no coating case reaches a maximum spectral radiance of 4.0 W/(m^2 nm sr).
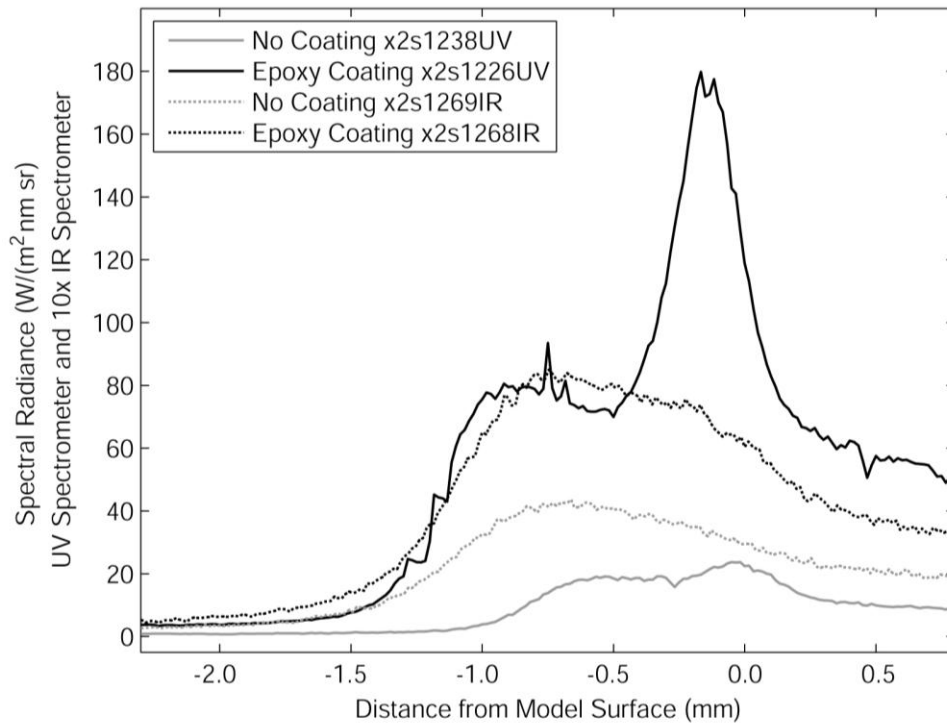

Fig. 3   Bow Shock Radiation Distribution with and without Ablation – UV and IR Spectrometers.

Although post-test measurements of the model would be desirable to determine quantify the amount of epoxy ablation that occurred, highly turbulent post- test time conditions in the expansion tunnel lead to further ablation as well as severe damage to the model. For this reason, post-test visual examination of the epoxy for material degradation, and shadowgraph or scale measurements to determine epoxy surface regression are not valid. The occurrence of ablation during the test time can only be measured by recording data during this period. Data from three independent instruments used in this study, the high speed camera, UV and IR spectrometers, all point to the occurrence of ablation during the test flow.

Influence of Oxygen

The influence of oxygen in air on radiation due to ablation was investigated by altering the shocklayer test gas from air to nitrogen. Figs. 11-12 show the emission spectra observed with the UV and IR spectrometers. When an epoxy coating is used with a nitrogen test gas, the radiance observed by the UV spectrometer (520 W/(m^2 nm sr)) is greater than with an air test gas (440 W/(m^2 nm sr)). However, the IR spectrometer observes a weaker radiance when an epoxy coating is used with a nitrogen test gas (75 W/(m^2 nm sr)) than with an air test gas (220 W/(m^2 nm sr)). This implies that oxygen in air acts to cool the shocklayer in the UV, possibly by an oxygen absorption mechanism, as suggested by Johnston 2008. In the IR, however, oxygen results in an increase in radiation. This may be due to oxygen atoms radiating more strongly than nitrogen ions at the shocklayer temperatures encountered.
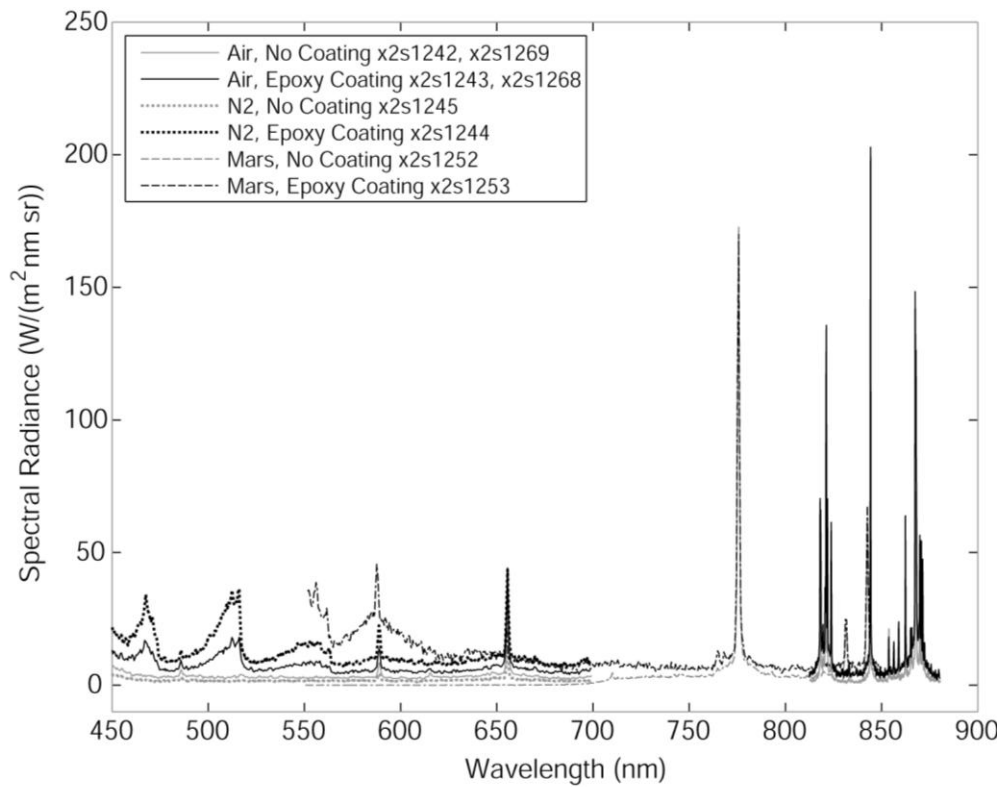
Fig. 4   Influence of Oxygen – UV Spectrometer.
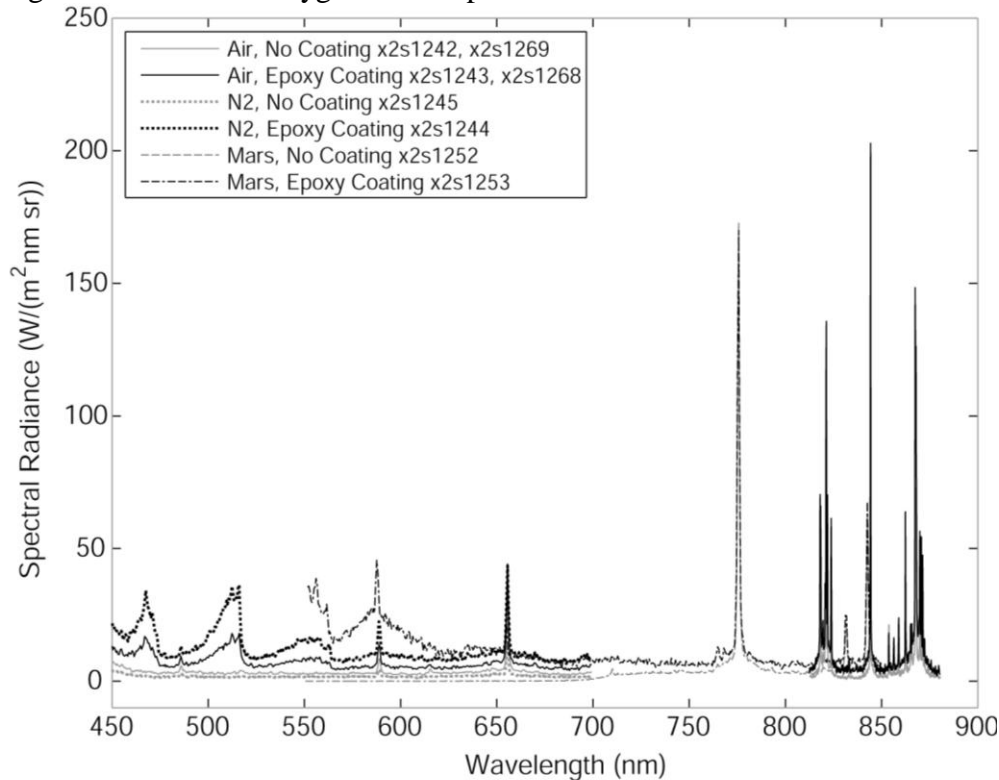
Fig. 5   Influence of Oxygen – IR Spectrometer.

The bow shock radiation distribution as observed by both spectrometers and high speed camera with and without an epoxy coating is given in Figs. 13-14. As in Fig. 10, the data in Figs. 13-14 are averages of emission spectra in the range 374 - 390 nm (UV spectrometer), 800 - 900 nm (IR spectrometer) and 400 - 700 (high speed camera). Regardless of test gas, the shock standoff distance with an epoxy coating is greater

than when no coating is employed. When no epoxy coating is used, the shock standoff distances are similar for air and nitrogen test gases, at approximately 1.0 mm. When an epoxy coating is used, the shock standoff distance is increased by 0.3 mm to 1.3 mm when a nitrogen test gas is used and by 0.5 mm to 1.5 mm when an air test gas is used.

The UV spectrometer observes similar spectral radiance levels when an epoxy coating is used with air and nitrogen test gases. An ablation layer peak spectral radiance is observed with both test gases, being greater with a nitrogen test gas (225 W/(m^2 nm sr)) than with an air test gas (175 W/(m^2 nm sr)). When no epoxy coating is used, the spectral radiance distribution is similar in shape for both air and nitrogen test gases, though is approximately three times stronger when a nitrogen test gas is used (peaking at 90 W/(m^2 nm sr)) than with air (peaking at 30 W/(m^2 nm sr)).
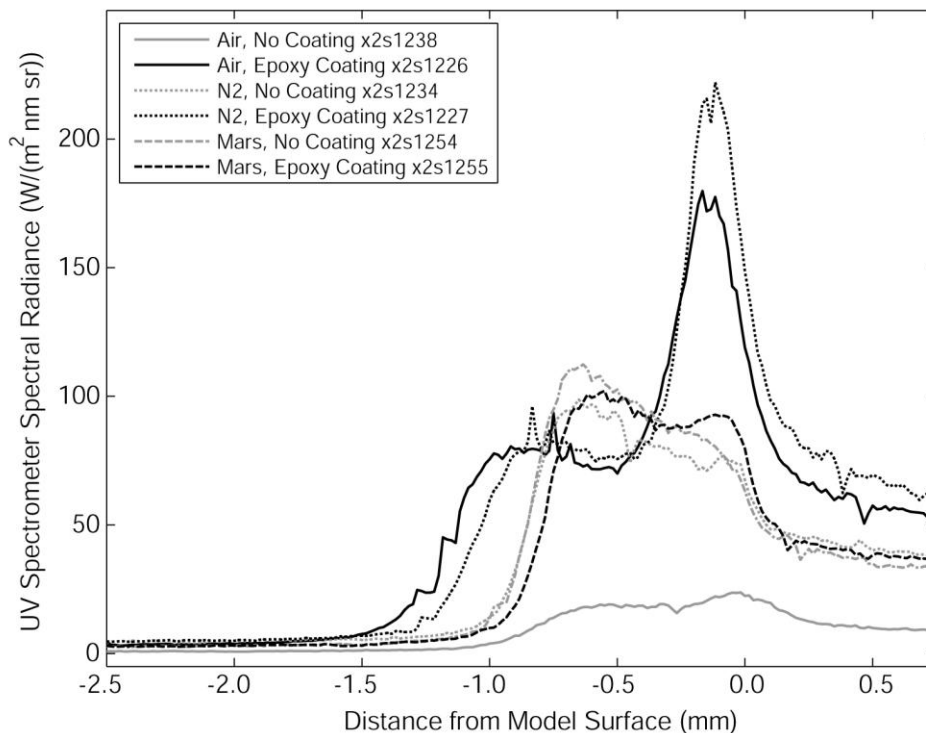

Fig. 6   Influence of Oxygen on Bow Shock Radiation Distribution – UV Spectrometer.

Summary/Conclusions

Additional studies of radiation from ablating shocklayer flows have been conducted in the expansion tube facility at The University of Queensland, following earlier proof-of-concept experiments showing the successful production of an ablating, radiating shock layer from an epoxy coating during the brief steady test time available.

In this study, radiation in ablating shocklayers over a scale Stardust model at 9 km/s was measured during the 80 μs steady test flow produced in a high enthalpy super-orbital expansion tunnel. The presence of an ablating shock layer when an epoxy coating is used with air and nitrogen test gases is shown by spectrometric and high speed camera data, and is in agreement with previous experimental results. Shock layer radiation is found to be strongest in the UV and visible portions of the electromagnetic spectrum, in both ablating and non-ablating shock layers. Shock layer radiation is greatly increased in ablating shock layers than in non-ablating shock layers when both air and nitrogen test gases are used.

A nitrogen test gas is thought to produce a higher temperature shock layer than when air is used, implying that oxygen in air has a cooling effect on shocklayer radiation, due to the dissociation of the oxygen molecules which occurs.

Shocklayer radiation in the near-IR is far weaker than that in the UV and consists of atomic, rather than molecular, transitions. As such, no distinct ablation layer is visible in the IR spectral data, however there is a doubling in radiance in the presence of an epoxy coating.

Suggestionsl for future study

A series of experimental measurements in the UQ expansion tube facilities (Morgan 19973, Neely 1994, Silvester 2004) is proposed whereby hypervelocity ablating shock layers will be created and probed with optical diagnostics to characterise their state and time development as accurately as possible. The results will drive a parallel program of theoretical analysis and numerical modeling, with the intention of validating procedures for the design of advanced spacecraft. The program will cover simulated atmospheres from Earth, Mars, Venus and Titan, and the gas giants. Experiments will also be run in the USQ Ludwieg tube and the RF plasma jet facility at Ecole Centrale to gain information about the ablation rates of substrates in the absence of surface heat transfer, and the radiating characteristics of the test gases.

The three atmosphere types chosen have very different characteristics, and the methodology of developing suitable TPS has to take this into account. The gas giants are totally dominated by radiative rather than convective heating, and the primary cooling role of ablative materials is to form a radiation absorbing layer of vapourised products above the surface of the vehicle. The dominant reaction is ionisation of the hydrogen atoms, as post shock dissociation is almost immediate due to the high associated speeds. The investigation here will look at the radiation absorbing capacity of vapourised and injected products, and the non equilibrium ionisation process which characterises the shock layer. Prior work has been done by the group on the ionisation (Higgins 2002), which will directly support the study.

  The carbon containing atmospheres (Mars, Venus and Titan) tend to radiate at relatively low speeds due to the formation of carbon products such as CO and CN, and therefore need protection systems designed to handle radiation at unexpected flight conditions. Work by Laux on the Huygens entry into Titan revealed the critical role of boundary layer absorption on heat transfer and engineering margins, and these are important area for further study. (The final entry of the probe into the atmosphere of Titan was only approved by mission controllers at the last minute, when calculations by Laux made when the vehicle was in flight just hours before entry showed that the expected heat transfer matched that of the ablative heat shield design, but with zero engineering safety factor. Errors had been discovered in the computations after launch of the Cassini mother craft which indicated the heat shield had been under-designed and would not survive entry, so they were considering cancelling the release of the Huygens probe to reduce risk to the primary Cassini mission. Both missions were successful, but as the probe was not instrumented, it is not known how close it came to failure. This illustrates the value of the sort of information which we hope to discover in such projects.) Carbon dioxide can also release oxygen, leading to surface reactions and increased ablation rate.

Air is a critical atmosphere, as it must be traversed at high speeds in both directions to perform tasks in space. Launch to space is a less challenging application than reentry due to the lower speeds (most launch paths effectively leave the atmosphere at speeds of about 1 km/sec, proposed scramjet flight paths call for atmospheric flight at speeds up to 4.5 km/sec which present special thermal control challenges in its own right), and is not considered in this proposal. Air has less powerful emitters than the other atmospheres, so radiation is not an issue until fairly high flight speeds of 11 km/sec and over. However, the presence of oxygen may lead to increased rates of ablation due to surface reactions, and it is proposed to study this effect in the presence of radiation, at speeds of 8 km/sec and over. The 'nitridation' reaction is also

important (Park 2006), where nitrogen atoms react with solid carbon to form CN, and is known to significantly enhance the ablation rate. (This reaction can also occur in the N2 dominated atmosphere of Titan, but the lower levels of nitrogen dissociation involved makes it less important in that application.)

The three parallel themes will use a similar methodology, and similar models and instrumentation to study what are related phenomena, but with strikingly different manifestations of the ablation process. The strong group of experienced partner investigators will be a great asset in providing the best possible supervision and advice to the students involved, and in advising on the ongoing technical direction of the experiments.

It is evident from Figure 1 that the interaction between shock layer species and ablation product species in the mixing layer plays a critical role in the ablative cooling process. Of special interest is how far from the wall the ablative products migrate, and what chemical composition results. Emission spectrometry will be the primary diagnostic. This has been used before on similar experiments, and found to be most effective on two dimensional flows, where signals integrated along a line of sight of uniform flow conditions can give accurate measurements of the radiation intensity at that point. In axisymetric flows, by using the Abel transformation and proper orientation of the spectrometer axis, it is possible to re-construct the variation of the emission spectra with radius throughout the axial plane being interrogated. An example of such a reconstruction is shown in figure 2, for an epoxy coated model which creates a layer of ablated products which can clearly be seen radiating as a separate layer between the bow shock and the wall. With the spectral profiles thus obtained, and using a numerical model of the radiating gas, it is also possible to estimate the concentrations of the radiating species, and the relevant temperatures (Potter 2008).

Knowing the surface ablation rate would significantly refine the comparison of theory and experiment. This is a difficult experimental step, as the flow duration is extremely short, and the source region is located in a very harsh, radiating environment. The ablation rate may be estimated from the local surface heating rate, (which can be measured to within about 20%), but that is intrusive, and requires assumptions which leave a large degree of uncertainty.

To address this problem, it is proposed to prepare models with prescribed depths of surface coatings, so that when the coating has been removed, the radiation signature will change measurably, thereby indicating the average ablation rate over the preceding test flow. This will be quite a complex task, and will have a dedicated PhD student assigned to it. The surface coating (probably less than 10 microns thick) must be mounted on a substrate with matching thermal properties.

In addition, a technique has been proposed by Buttsworth to monitor the surface temperature directly. Ablation is driven by rises in the surface temperature, so its measurement would be very useful. The epoxy surface will have a temperature ~ 500K plus and emit strongly in the infrared (IR) while a steel surface will be at ~ 300K and emit weakly. The signal from an infrared (IR) sensor aimed at a region on the model surface is the sum of the IR emission from the intervening gaseous flow and the surface IR emission. Thus the difference in signal from an IR sensor aimed at the epoxy surface and one aimed at a steel surface can be used to infer the epoxy surface temperature rise. This is so provided the intervening gaseous flows and the optical geometries are the same in the two cases. A similar technique has been successfully used on models in a cold 'gun tunnel', flow where radiation from the test gas was not important, and we are confident it can also be made to work in this more challenging application.

In the quasi steady equilibrium situation achieved in flight, the start of the molten layer may be under the surface, and the evaporation rate will be a function of the surface temperature of the melt, and the partial pressure of evaporated species at the liquid-vapour interface. This partial pressure will depend on the processes taking place in the external flow, and entrainment of evaporated species into the boundary layer

will increase the rate of evaporation. Depending on the local temperature and static pressure, the liquid surface may be boiling under conditions of high heat transfer. However, the resins used in TPS do not exhibit clearly defined 'boiling' and 'melting' points, and the different components are driven off over a range of temperatures in a finite rate process commonly called 'outgasing'. The temperatures and ablation rates will equilibrate to give a steady flow balance between the external heat input, and the enthalpy convected away from the surface, including chemical and thermal terms, and those relating to changes of phase. Under such conditions, the surface will be slowly receding, so the situation cannot be truly described as steady, but the effect of the low speed transient terms become negligible, and a quasi-steady approach adequately captures the process. In high speed reentry, the associated temperatures of such a situation are high, with the exposed surfaces of ablators typically being in the range from 2000 to 3000K.

In a transient process created in the expansion tubes the mechanisms are slightly different. Firstly, the initial pulse of heat penetrates into the exposed surface, volatiles begin leaving the surface a finite time later, and ablation starts. Up to this time, the surface heat transfer is conducted into the substrate, heating a growing region of the model, approximately 10 microns deep for the relevant timescales.

Once the surface gets hot enough, and volatiles begin to outgas from the surface, the energy balance becomes more complex, with the absorbed heat supplying both the convected flux away from the wall, and the growth of the transiently heated and possibly melted zone underneath. However, at the vapourising surface, the situation is locally similar to steady flow, (although at very different temperatures) in that the instantaneous rate of out-gassing is the same function of the surface temperature achieved, and the partial pressure of evapourated species at the interface. For this reason, the expansion tube experiments proposed here reproduce important aspects of what happens in flight, if the relevant heat transfer rates and boundary layer conditions are created.

To study this phenomenon in more detail, an additional series of cold tests are proposed whereby a preheated sample of ablator at the temperature of interest is exposed to a low enthalpy hypersonic flow, with the total temperature set so that no aerodynamic heat transfer is produced. Under these conditions, no radiation is produced from the test gas either, so the surface temperature can be held almost constant, and it represents an ideal benchmark situation to examine the process over a wide range of conditions. Due to the long test time of this facility, and the cleanliness of the flow which avoids the surface damage caused in the expansion tubes, it will be possible to measure the ablation rates accurately, and quantify the process in a well controlled situation. This understanding will be very useful for interpreting the data we get when the ablation is driven from the aerodynamic input, rather than embedded electrical heaters in the model.

The ablative situation created in the laboratory is fundamentally different to that in reentry flight, in that an unsteady stream of vapourised products is released from a thin surface layer through a transient heating process. In flight, a quasi steady balance exists between the mass and heat transfer processes, and very high 'equilibrium' surface temperatures are reached. The physical mechanisms pertaining to flight are present in the laboratory, but the dynamics and boundary conditions are different, and these have to be properly understood to get meaningful output from the experiments

The atmospheres of interest:
Gas Giants (Jupiter, Neptune, Saturn, Uranus)
Entry into the atmospheres of the gas giants presents an extreme challenge to TPS, as the speeds reach values up to 50 km/sec, (Park 2008). The atmosphere consists primarily of ~90% H2 in He. The H2 dissociates very quickly after the shock, and ionisation of the H atoms occurs initially through heavy particle collisions. When sufficient electrons are released, they become the primary cause for further ionisation, through a two step process of excitation to the first excited state, followed by ionisation on subsequent collisions. The ionisation energy of the Helium is such that not much of it ionises, and its

primary role is to initialize the ionisation of the H atoms. These speeds exceed those that can be attained in facilities for reproducing aerodynamic flows. However, the primary non equilibrium process of interest is the ionisation of Hydrogen atoms in the shock layer, and it has been shown (Stalker 1998, Higgins 2002, Inger 2002, 2003) that by substituting Ne for the He found in the atmospheres of all the gas giants, a similarity can be obtained with flight at speeds of the order of 10km/sec, because the heavier Ne atoms reach the same temperature as the helium atoms would do at the higher speeds. The Ne atoms also have a high ionisation energy, so they play the appropriate role of non reacting collision partners. Previous work in X2 has investigated this effect through measurements of shock standoff on blunt bodies, and has confirmed the similarity by use of an analytical model based on Dahmkohler numbers for the ionisation process, (Inger 2002,2003).

For the purposes of this new study, we want to investigate the effects of the gas giant atmospheres on the ablation process. Jupiter entry is a classic case of radiation driven heat transfer, with radiation contributing over 95% of the total surface heating, so we will need to understand the radiating environment, and specifically to know what effects the Ne-He substitution will have. Another interesting feature of Jupiter entry is that the cloud of abating products acts as an energy absorbing layer between the shock layer and the surface. To investigate this phenomena, surface mounted instrumentation will be required, so we can measure the heat transfer to the model with and without ablative products. For this set of experiments, we will artificially inject a flow of simulated products into the shock layer, and measure the subsequent surface heat transfer through total radiation probes (Capra 2007), and spectrometers fed by fibre optics embedded in the surface.

To provide benchmark calibration data from equilibrium flow, and to understand the differences between H2/He and H2/Ne radiating mixtures, an important set of parallel experiments will be performed in the 50kw RF plasma jet facility at Ecole Centrale (EC). EC are providing time on the facility as an in-kind contribution, and it is proposed that another co-tutelle PhD student working at both EC and UQ will perform the experiments. This will provide data for calibration of the radiative collision models needed to simulate the process, and it will also be used to calibrate the absorption characteristics of the injectants used in the expansion tube experiments at UQ. The latter measurement can be obtained by passing a flow of methane between the radiating H/Ne flow, and the spectrometers. Currently, methane is the preferred injectant, due to its low molecular weight, but a heavier hydrocarbon may eventually be needed to give sufficient absorption in the uv spectrum where most of the heating occurs.

Earth

The situation for entry into the earth's atmosphere of air is physically quite different from the other planets, because of its high oxygen content. This has the effect of providing free oxygen which can react chemically with the surface material, whilst the low level of carbon containing species reduces the amount of radiation from the shock layer, and shifts its significance to the shorter wavelength spectrum. A major challenge for the space shuttle was to develop a reusable surface insulation for the hot spots on the nose and wing leading edges that could resist erosion from the high temperature oxygen in the flow. This was achieved by deposition of a surface layer of silica on the RCC composite, which protected the carbon structure from oxidation. Of the three surface reaction types associated with carbonaceous ablators, only the gas-solid interaction will be considered in this study. The surface temperatures reached in the experiments are not likely to be high enough to induce much sublimation of the solid char, and catalytic recombination of molecular oxygen and nitrogen is known not to be important on ablators. For the higher speed regime of ablative systems, the interaction of the oxygen with the particulate components of the surface is very important, and full protection of exposed surfaces from oxidation has not yet been achieved. The nitridation reaction is also an important surface reaction responsible for significant mass removal through ablation, but does not change heat transfer much due to low heat of formation (Park 2010). The products of these two

reactions are CO and CN, both of which have recognizable radiation footprints, and their release will be clearly indicated from the spectrometry measurements.

To study surface chemistry effectively, temperatures above 1000K have to be created. We have demonstrated the ability to generate ablative layers formed from the volatiles contained in TPS substrates with temperatures of the order of 600K (D'Souza 2010), and that technique forms an important part of this proposal. However, the thermal products of the resins are rather high with values typically of the order of $600 \, Jm^{-2}K^{-1}s^{-0.5}$ (the square root of the product of the density, conductivity and specific heat determine how hot a surface will get when exposed to impulsive heating of short duration, and is colloquially know as the 'thermal product'), and temperatures required to study surface chemistry cannot be reached within the run times of our facilities using the epoxy and phenolics resins.

Alternative surface materials are available which we believe would enable us to reach temperatures high enough to study surface reactions. These include the use of natural cork (cork has been used as an insulator on many space vehicles, thermal product 167, ignition temperature 600K), MA25 (the insulator used on the space shuttle external tanks, the damage from fragments of which was blamed for the loss of the Columbia, thermal product 235, ablation temperature 780K), and the 'super-lightweight' ablators such as SLA561V used of the Mars 'Pathfinder' mission (thermal product 120, ablation temperature 830K). These materials should get between about 3 and 5 times as hot as the previous materials we have tested on X2, and with the longer running times available when we use X3 for these purposes, the regime of surface reaction will be well simulated. Of special interest in these experiments will be the formation of species produced by the reaction of the hot structure with the atmospheric oxygen, which will be examined by emission spectrometry. In addition, the SLA561V can be baked in an oven before testing to drive out the volatiles, and reproduce the composition of the surface of a vehicle at a stage of a flight path when the surface layer of volatiles has been vapourised, and the flow is in contact with an exposed char.

The carbon containing atmospheres (Mars, Venus, Titan)

Carbon is present in atmospheres of the solar systems primarily in the form of carbon dioxide (Mars and Venus), and Methane (Titan). The heavy carbon containing molecules dissociate easily, which leads to very high density ratios across the bow shocks and small shock standoff distances (especially for Mars and Venus). In addition, the carbon species formed are strong radiators, and radiation may be the primary form of heat transfer at much lower speeds than would be expected either for Earth or the gas giants. For instance, radiation from the CN molecules formed at Titan by reaction of the carbon released from dissociation of the small (1.5%) CH4 content with the remaining nitrogen dominates heat transfer at a speed of 6 km/sec, whilst for moon return to earth at a speed of 11.2 km/sec radiation is a secondary issue (though still important, at 20% of the total).

In previous studies, we have reproduced superorbital flows relating to these atmospheres, and have made some measurements of the radiative heating background under which the ablation will be occurring (Wegner 2001, Gollan 2004). The purpose of these experiments will be to study the ablative processes in a controlled situation, and use the diagnostics to quantify the important parameters of the flow.

REFERENCES

P. A. Gnoffo, K. J. Weilmuenster, I. I. Hamilton, D.R. Olynick, and E. Ventatapathy. Computational aerothermodynamic design issues for hypersonic vehicles. A.I.A.A. Journal of Spacecraft and Rockets, 36(1):21–43, 1996.

B. James, M.Munk, and S.Moon. Aerocapture technology project overview. In 39th Joint Propulsion Conference and Exhibit, Paper 2003-4654, Huntsville, AL., July 2003. A.I.A.A.

R. G. Morgan. A review of the use of expansion tubes for creating superorbital flows. In 35th Aerospace Sciences Meeting and Exhibit, Paper 97-0279, Reno, NV., January 1997. A.I.A.A.

A. J. Neely and R. G. Morgan. The superorbital expansion tube concept, experiment and analysis. The Aeronautical Journal, 98(973):97–105, 1994.

M. Wegener, M. Sutcliff, R. G. Morgan, T. J. McIntyre, and H. Rubinsztein-Dunlop. Diagnostics of a range of highly superorbital carbon dioxide flows. In 39th Aerospace Sciences Meeting & Exhibit, Paper 2001-0304, Reno, NV., January 2001. AIAA.

R. J. Gollan, P. A. Jacobs, S. Karl, and S. C. Smith. Numerical modelling of radiating superorbital flows. Australian & New Zealand Industrial and Applied Mathematics Journal, 45:C248–C268, 2004.

S. Karl. Simulation of radiative effects in plasma flows. DC report, von Karman Institute for Fluid Dynamics, 2001.

G.J. Elbert and P. Cinnella. Axisymmetric radiative heat transfer calculations for flows in chemical non-equilibrium. AIAA Paper 93-0139, 1993.

D. L. Cauchon. Radiative heating results from the Fire II flight experiment at a reentry velocity of 11.4 km/sec. Technical Memorandum X-1402, NASA, 1967.

E. S. Cornette. Forebody temperatures and calorimeter heating rates measured during project Fire II reentry at 11.35 km/sec. Technical Memorandum X-1305, NASA, 1966.

R. R. Ried, W. C. Rochelle, and J. D. Milhoan. Radiative heating to the Apollo command module:Engineering prediction and flight measurement. Technical Memorandum Z-58091, NASA, 1972.9

B. R. Capra, P. Leyland, and R. G. Morgan. Subscale testing of the Fire II vehicle in a superorbital expansion tube. In 42nd AIAA Aerospace Sciences Meeting and Exhibit, Paper 2004-1298, Reno, NV., January 2004. A.I.A.A.

P. A. Jacobs, T. B. Silvester, R. G. Morgan, M. P. Scott, R. J. Gollan, and T. J. McIntyre. Superorbital expansion tube operation: Estimates of flow conditions via numerical simulation. In 43rd AIAA Aerospace Science Meeting and Exhibit, AIAA-Paper-2005-0694. American Institute of Aeronautics and Astronautics, January 2005.

T. B. Silvester, R. G. Morgan, and P. A. Jacobs. Skin friction measurements in a duct in the X3 superorbital expansion tube. In 40th AIAA/ASME/SAE/ASEE Joint Propulsion Conference and Exhibit, AIAA-Paper-2004-3551, July 2004.

B. Laub, MJ Wright, E Venkatapathy.Thermal Protection System (TPS) Design and the relationship to atmospheric entry requirements. 06/21-22. 6th International Planetary Probe Workshop, Atlanta. Short Course on Extreme Environmental Technologies, 2008

C Park. Calculation of stagnation-point heating rates associated with Stardust vehicle. Journal of Spacecraft and Rockets, Vol 44, No 1 January- February 2007.

C Park. Non equilibrium ionisation and radiation in H2-He mixtures. AIAA 2010-814. 48th AIAA Aerospace Sciences Meeting, Orlando, Florida, 4 to 7 January 2010.

Christophe Laux, Michael Winter, James Merrifield, Arthur Smith, Philippe Tran, Influence of Ablation Products on the Radiation at the Surface of a Blunt Hypersonic Vehicle at 10 km/s, AIAA-2009-3925 41st AIAA Thermophysics Conference, San Antonio, Texas, June 22-25, 2009

G.R.Inger, C. Higgins, R.G.Morgan. Shock standoff on hypersonic bodies in non-equilibrium gas flows. April/June 2002 AIAA J Thermo. Phys and Heat Transfer.

Inger, GR; Higgins, C; Morgan, R. Generalized Nonequilibrium Binary Scaling for Shock Standoff on Hypersonic Blunt Bodies. Journal of Thermophysics and Heat Transfer. V17, No 1. 2003.

J.J. Na, C. Park, K.S. Chang, and J. Muylaert. Assessment of the interaction of radiation, convective heating, and ablation in the "RADFLIGHT" re-entry experiment. *6th European Synposium on Aerothermodynamicsfor Space Vehicles,* ESA SP-659, 2008.

B.R. Capra. *Aerothermodynamic simulation of subscale models of the FIRE II and Titan Explorer vehicles in expansion tubes.* PhD thesis, University of Queensland, St. Lucia, Australia, 2007.

Stalker,R.J. Edwards, B.P.,(1998) Hypersonic Blunt Body Flows In Hydrogen-Neon Mixtures, J.Spacecraft & Rockets, V35, No 6, 1998, pp 729-735.

D'Souza MG, Eichmann TN, Mudford NR, Potter DF, Morgan RG, McIntyre TJ, Jacobs PA (2009) Observation of an Ablating Surface in Expansion Tunnel Flow, Submitted to the AIAA Journal, September, accepted subject to editorial corrections.

Higgins, C.E., Inger, G.R., Morgan, R.G. (2002) "Shock Standoff on Hypersonic Blunt Bodies in Multi-Temperature Ionizing Nonequilibrium Gas Flows", *8th AIAA Joint Thermophysics and Heat Transfer Conference*, St Louis MO, June 24-26, Paper 2002-3312.

RG Morgan. Heat transfer studies in high temperature gases. D. Phil Thesis. Oxford University 1976

Potter, D., Eichmann, T., Brandis, A., Morgan, R., Jacobs, P., McIntyre, T., "Simulation of radiating CO2–N2 shock layer experiments at hyperbolic entry conditions," AIAA Paper: AIAA-2008-3933, 40th Thermophysics Conference, Seattle, Washington, June 23-26, 2008

Jenniskens, P. (2005). *Hypervelocity Re-entries.* Available at http://reentry.arc.nasa.gov.

Milos, F.S. (1997). *Galileo Probe Heat Shield Ablation Experiment*. Journal of Spacecraft and Rockets. **34**(6).

Winter, M. & Herdrich, G. (2008). *Heat Shield Temperatures and Plasma Radiation obtained from Spectroscopic Observation of the STARDUST Re-Entry in the Near UV*. 46th AIAA Aerospace Sciences Meeting and Exhibit, AIAA2008-1212, Reno, USA.

Johnston, C., Gnoffo, P., & Sutton, K. (2008). *The Influence of Ablation on Radiative Heating for Earth Entry.* 40th Thermophysics Conference, AIAA2008-4107, Seattle, USA.

Olynick, D., Chen, Y.K. & Tauber, M.E. (1999). *Aerothermodynamics of the Stardust Sample Return Capsule*. Journal of Spacecraft and Rockets. **36**(3).

Park, C. (2007). *Calculation of Stagnation-Point Heating Rates Associated with Stardust Vehicle*. Journal of Spacecraft and Rockets. **44**(1).

Stackpoole, M., Sepka, S. & Cozmuta, I. (2008). *Post-Flight Evaluation of Stardust Sample Return Capsule Forebody Heatshield Material*. 46th AIAA Aerospace Sciences Meeting and Exhibit, AIAA2008-1202, Reno, USA.

D'Souza, M.G., Eichmann, T.N., Mudford, N.R., Potter, D.F., Morgan, R.G., McIntyre, T.J. & Jacobs, P.A. (2010). *Observation of an Ablating Surface in Expansion Tunnel Flow*. AIAA Journal. **48**(7).

Morgan, R.G., McIntyre, T.J., Jacobs, P.A., Buttsworth, D.R., Macrossan, M.N., Gollan, R.J., Capra, B.R., Brandis, A.M., Potter, D.F., Eichmann, T.N., Jacobs, C.M., McGilvray, M., Van Diem, D. & Scott, M.P. (2006). *Impulse Facility Simulation of Hypervelocity Radiating Flows*. 2nd International Workshop on Radiation of High Temperature Gases in Atmospheric Entry, ESA, The Netherlands.

Morgan, R.G., Sasoh, A., Littleton, B., Bishop, A., McIntyre, T.J., Hoogland, J.D. & Gardner, A.D. (1999). *Simulation of Ablative Mixing Layers in Superorbital Flows*. 22nd International Symposium on Shock Waves, University of Southampton, Southampton, UK, pp. 727-732.

Hunt, D.C. (2002). *Measurement of Ablation in Transient Hypersonic Flows*. M.Sc. Thesis, The University of Queensland, Australia.

Zoby, E. (1968). *Empirical Stagnation-Point Heat-Transfer Relation in Several Gas Mixtures at High Enthalpy Levels*. NASA Langley Research Center, TN D-4799.

Schultz, D.L. & Jones, T.V. (1973). *Heat-Transfer Measurements in Short Duration Hypersonic Facilities*. AGARD, AGARDograph AG-165.

Potter, D.F., Eichmann, T.N., Brandis, A., Morgan, R.G., Jacobs, P.A. & McIntyre, T.J. (2008). *Simulation of radiating CO2-N2 shock layer experiments at hyperbolic entry conditions*. 40th AIAA Thermophysics Conference, Seattle, USA.

Gordon, S. & McBride, B.J. (1994). *Computer program for calculation of complex chemical equilibrium compositions and applications. Part 1: Analysis*. NASA Reference Publication 1311, USA.

eFunda. (2009). *Engineering Fundamentals: Properties of Epoxy*. Available at http://www.efunda.com.

Richardson, M.J. (2008). *2.3.6 Specific Heat Capacities*. National Physical Laboratory. Available at http://www.kayelaby.npl.co.uk.

Buttsworth, D., D''Souza, M.G., Potter, D.F., Eichmann, T.N., Mudford, N.R., McGilvray, M., McIntyre, T.J., Jacobs, P.A. & Morgan, R.G. (2010). *Expansion Tunnel Radiation Experiments to Support Hayabusa Re-entry Observations*. 48th AIAA Aerospace Sciences Meeting and Exhibit, AIAA-2010-0634.

Laux, C., Andreasson, J. & Risberg, J. (2006). *SpecAir*. Radiation spectra software package, Ver.2.2.0.0, EM2C Lab., Ecole Centrale Paris. Available at http://www.specair-radiation.net.

Kattari, G.E. (1965). *The Effect of Simulated Ablation-Gas Injection on the ShockLayer of Blunt*

Appendix

A.　　Personnel Supported:

The bulk of the experimental work reported in this document was performed by Mary D'Souza, as part of her PhD studies at The University of Queensland (UQ). Her supervisory team during the project were Richard Morgan and Tim McIntyre from UQ, and Neil Mudford from the Australian Defense Force Academy. Neil Mudford performed the analysis to reconstruct the axi symmetrical radiation intensity fields from the 2D recorded data. Troy Eichmann assisted with the instrumentation and experimental measurements. Dan Potter and Peter Jacobs assisted with numerical analysis of the expansion tunnel flow fields. David Buttsworth and Russell Boyce were involved in developing the methodology and planning throughout the program.

B.　　Publications:

D'Souza, M.G., Eichmann, T.N., Mudford, N.R., Potter, D.F., Morgan,R.G., McIntyre,T.J., Jacobs,P.A., "Observation of an Ablating Surface in Expansion Tunnel Flow", AIAA Journal, Vol. 48, No. 7, 2010.

D'Souza, M.G., Eichmann, T.N., Mudford, N.R., Potter, D.F., Morgan, R.G., McIntyre, T.J., "An Experimental Investigation of Radiation over an Ablating Stardust Model at 9.8 km/s", IAC 2010 paper

D'Souza, M.G., Eichmann, T.N., Potter, D.F., Mudford, N.R., Morgan, R.G., McIntyre, T.J., "Radiation Measurements of an Ablating Shocklayer around a Stardust Model near Peak Heating", 3rd RHTG Workshop, Lausanne, Switzerland, 2010

B.　　Interactions:

The interest generated by the experiments performed under the grant led to the formation of a group involving the Department of Aeronautics and Astronautics AFIT, Ecole Centrale (Paris), DLR Gottingen, UQ and ADFA to further study ablative shock layers, and prepare follow-on funding applications. Personnel

from AFIT visited UQ in 2009 during the experimental program, and will be performing numerical analysis on the data. Richard Morgan visited collaborators at AFIT in May 2010, and gave a presentation on the work. During his sabbatical secondment in 2010, R Morgan gave invited presentations on the work at Institutions in India, China, Switzerland, Germany, France and USA. Several members of the group attended the 3rd RHTG Workshop, Lausanne, Switzerland, 2010 and gave presentations on the work that were well received.